

Gas-Phase Potassium Binding Energies of MALDI Matrices: An Experimental and Theoretical Study

Juan Zhang, Evgueniya Dyachokva,[†] Tae-Kyu Ha, Richard Knochenmuss,[‡] and Renato Zenobi*

Department of Chemistry, Swiss Federal Institute of Technology (ETH), ETH–Hönggerberg, CH-8093 Zürich, Switzerland

Received: January 29, 2003; In Final Form: June 6, 2003

Gas-phase potassium binding free energies of four aromatic molecules, which are used as matrices in the matrix-assisted laser desorption/ionization (MALDI) mass spectrometry, were determined experimentally by the ligand-exchange equilibrium method in a Fourier transform ion cyclotron mass spectrometer (FT ICR MS). The matrices studied were 2,5-dihydroxybenzoic acid, 2,4,6-trihydroxyacetophenone, *trans*-3,5-dimethoxy-4-hydroxycinnamic acid, and 1,8,9-trihydroxyanthracene. In addition to the experimental values, we also present quantum chemical results obtained by the density functional theory (DFT) at the 6-31+G* level. The gas-phase potassium binding free energies of the MALDI matrices studied in this work are in the range of 90–105 kJ mol⁻¹.

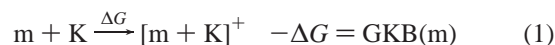
1. Introduction

Investigations of alkali ion affinities/basicities have been attracting increasing attention due to the great significance of alkali metal cationization for the analysis of polymers by matrix-assisted laser desorption/ionization mass spectrometry (MALDI MS).^{1–9} Potassiated quasi-molecular ion signals are often observed in MALDI mass spectra in addition to protonated and sodiated signals. A gas-phase ion formation mechanism was supported by several studies of cationization in MALDI MS.^{7,10–13} Other investigations consider metal cation transfer as one of the important secondary ion formation processes in MALDI plume; these processes are largely under thermodynamic control.^{14–18} These works suggested that thermodynamic values such as metal ion affinities/basicities of analytes as well as matrices are important for clarifying the cationization mechanism in MALDI. Values of the metal ion cation binding energies of the MALDI matrices are, however, largely unknown, in particular, for potassium. Gas-phase sodium cation binding free energies of some common MALDI matrices have been determined experimentally in our laboratory. Theoretical studies of the gas-phase interaction between sodium cation and MALDI matrices have been reported by Ohanessian¹⁹ and our laboratory.²⁰

Gas-phase potassium affinities/basicities (GKA/GKB) (reaction 1) of small organic molecules (M) can be determined by the equilibrium method,^{21–25} the kinetic method,^{26,27} threshold collision-induced dissociation (CID),^{28–33} and by theoretical calculations.^{31–40} Among these methods, only the CID method introduced by Armentrout et al. (see for example ref 41) gives absolute experimental values for the metal ion binding energy. Binding energies obtained by the kinetic and equilibrium methods are strongly dependent on the reference values used in the data evaluation. Therefore, the relative metal ion binding

energies of a series of molecules studied are more precisely determined than the absolute values by these methods. In this work, we present the gas-phase potassium basicities of MALDI matrices determined by using the ligand-exchange equilibrium method.

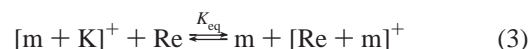
The gas-phase potassium basicity of a molecule M is defined as the negative value of the potassium binding free energy (reaction 1).



The determination of gas-phase sodium basicities of common MALDI matrices by the equilibrium method in a FT ICR MS has been described before.⁴² The gas-phase potassium basicity of a molecule m is given by

$$\text{GKB}(m) = \text{GKB}(\text{Re}) - RT \ln K_{\text{eq}} \quad (2)$$

where K_{eq} is the equilibrium constant of the gas-phase potassium transfer reaction (reaction 3) between the potassiated matrix and a reference base (Re) with known GKB.



For the quantum chemical study of potassium cation complexes, many different methods and basis sets have been employed. Most of these studies applied ab initio methods using Hartree–Fock (HF) wave functions. Although the most reliable method for the calculation of the energies is, as generally acknowledged, the Gaussian-2 (G2) theory,⁴³ many other theoretical methods that are less time-consuming have been employed and tested. Second-order perturbation theory (MP2) with modified basis sets was used for studying the interaction of potassium and glycine in the gas phase.^{36,40,44} Hill et al. have studied alkali metal cation binding to a series of small organic molecules and crown ethers using HF with MP2.^{35,37,45,46} For potassium and other heavier metal ions, they have used the metal effective core potentials by Hay and Wadt (ECPs).⁴⁷ Both CID experiment

[†] Present address: Institute of Energy Problems of Chemical Physics, Russian Academy of Science, 117829, Moscow, Russia.

[‡] Present address: Novartis Pharma AG, WSJ-503.1104, CH-4002 Basel, Switzerland.

and the MP2 theory were performed for studying the absolute alkali metal ion binding energies of several azines,³¹ the noncovalent interactions of the metal ions with some nucleic acid bases,⁴⁸ and the influence of substituents on cation- π interactions.³³ A reasonable agreement was obtained between CID experiments and the ab initio results. The calculated values were found to be 16 ± 8 kJ mol⁻¹ lower than the experimental values. A poor agreement was obtained in the investigation of the potassium selectivity of 18-crown-6 by using the restricted Hartree-Fock (RHF) with standard basis sets (3-21G and 6-31+G*) and relativistic ECPs.⁴⁹ A comprehensive ab initio study of alkali metal cation-water clusters using a series of basis sets has been done by Feller and co-workers.⁵⁰ Good agreement were found for small clusters (up to four water molecules) when MP2 was applied (with up to 11% deviation). They also found that reliable binding energies were obtained when 6+31G* basis sets were applied with counterpoise correction.

In the past few years, density functional theory (DFT) methods have attracted great interest and attention. In contrast to other high level ab initio methods, DFT functionals provide less drastic scaling of frequency. For the computation of ionization potentials and electron affinities, the performance of density functional methods was satisfactory in comparison with the G2 theory.⁵¹ The cation- π effects in the complexation of Na⁺ and K⁺ with aromatic amino acids in the gas phase has been studied by Ryzhov et al. using the DFT methods.²⁷ Feller et al. have compared the MP2, RI-MP2, and DFT methods for the study of the structure and binding energy of K⁺-ether complexes.⁵² They found that even by classical electrostatics model, e.g., cation-ether interactions, the accuracy of density functional techniques is quite sensitive to the choice of functionals. Ohanessian has studied the interaction of the sodium ion with MALDI matrices by using Hartree-Fock wave functions with second-order perturbation theory, and the DFT method.¹⁹ In general, the DFT method gives sufficiently accurate results. The latest experimental and theoretical study of the potassium cation complexes with ammonia shows that both MP2 and B3LYP methods can reproduce the experimental results accurately, while by using the effective core potentials, poor agreement between the experimental and theoretical values was shown.³² A study of competing sites for metal cation binding to phenol was accomplished by using the DFT method.⁵³ In this work, different DFT functionals were compared. Only minor differences of the metal cation binding to oxygen were found when using different DFT functionals.

The DFT method has also been employed for studying the thermochemical properties of MALDI matrices, including ionization energies of matrices, sodium binding energies, proton and electron affinities of neutral molecules, as well as proton affinities of deprotonated molecules.^{19,20,54-56} In these works, the performance of the DFT method was quite satisfactory for the accurate evaluation of thermochemical data. In this work, we used the B3LYP functional for evaluating potassium binding to MALDI matrices.

2. Experimental Procedures

All experiments were performed on a Fourier transform ion cyclotron resonance mass spectrometer (FT ICR MS) with an opened elongated cylindrical cell. The instrument is equipped with a 4.7 T superconducting magnet (Bruker, Fällanden, Switzerland) and Odyssey data acquisition electronics (Finnigan, Madison, WI). A Nd:YAG laser (Minilite ML-10, Continuum, CA) operated at 355 nm was employed for laser desorption.

Matrix was dissolved in ethanol/water and mixed with an aqueous solution of potassium chloride in a molar ratio of ca. 1:1. This mixed matrix-salt solution was dropped on a stainless steel sample carrier and allowed to dry at room temperature. This dried-droplet procedure was repeated several times until there was a good crystal layer. The sample was placed in front of the cell at 2 cm distance. Using laser desorption, potassium matrix ions were generated in the gas phase, and subsequently isolated after a cooling period. Finally, the potassium matrix ions were allowed to react with a reference base, dimethoxyethane. Sublimation of the solid sample gave a constant partial pressure of neutral matrix molecules [m]. This was verified by employing electron impact ionization (EI). Vapor of dimethoxyethane was introduced through a leak valve. The experiments were carried out at 298 K. The pressure during the experiment was typically 1.0×10^{-8} mbar. Spectra were summed over 10 laser shots and taken with various reaction times until the reaction approached equilibrium. The ratio of ions ([Re + K]⁺/[m + K]⁺) were obtained from mass spectra. The vapor pressure of the MALDI matrices studied in this work are rather low. This causes difficulty in measuring the absolute matrix partial pressure. We therefore measured the ratio of two neutrals ([m]/[Re]) by electron impact ionization EI, eliminating the uncertainty of the measurements of the absolute partial pressure in the FT ICR cell. Details have been described in a previous publication.⁴² The measured neutral ratios were corrected by applying known pressure gauge sensitivity factors.⁴² For error analysis, we have applied a conservative estimation of the uncertainty of the sensitivity factors ($\pm 50\%$). To evaluate the error of the final results, the standard deviation of the data points, obtained from five repetitions of each experiment, together with the estimated uncertainty of the sensitivity factors were taken into account.

Matrices were purchased from Fluka (Buchs, Switzerland): 2,5-dihydroxybenzoic acid (DHB), *trans*-3,5-dimethoxy-4-hydroxycinnamic acid (sinapinic acid, SA), 1,8,9-trihydroxyanthracene (dithranol), and 2,4,6-trihydroxyacetophenone (THAP).

3. Computational Details

Density functional theory using the combined Becke's three-parameter exchange functional and the gradient-corrected functional of Lee, Yang, and Parr (B3LYP functional)⁵⁷⁻⁵⁹ was employed throughout in this work for the calculation of the equilibrium geometries and the harmonic vibrational frequencies at the 6-31+G* level. The optimized geometries of different metal complex conformers were compared in order to find the most stable conformation. The binding energies were computed as the reaction energy of reaction 1. The calculations were accomplished at 1.0 atm and 298.15 K for the reactants and products in the reaction 1. Binding energies were corrected for the basis set super position errors (BSSE) using the counterpoise procedure.⁶⁰ All the calculations were done using the Gaussian98 package.⁶¹

4. Results and Discussion

The gas-phase potassium basicities of four MALDI matrices obtained experimentally are given in Table 1. For comparison, the gas-phase sodium basicities of the four matrices obtained previously⁴² are also given. The gas-phase potassium binding energies obtained computationally are presented in Table 5. The computed results are compared with the experimental data for each matrix individually.

4.1. Experimental Results. Figure 1 shows the FT MS spectra taken during the gas-phase potassium transfer reaction

TABLE 1: Gas-Phase Potassium Basicities (GKB) of MALDI Matrices Measured Experimentally at 298 K^a

matrices	K ⁺		Na ⁺	
	GKB	relative values	GNaB	relative values
SA	104 ± 4	10	159 ± 2	9
DHB	99 ± 2	5	158 ± 3	8
THAP	97 ± 4	3	154 ± 2	4
dithranol	94 ± 3	0	150.5 ± 0.5	0

^a The relative values are anchored to that of dithranol. All energies are given in kJ mol⁻¹. Values of the gas-phase sodium basicities (GNaB) are taken from our previous work.⁴²

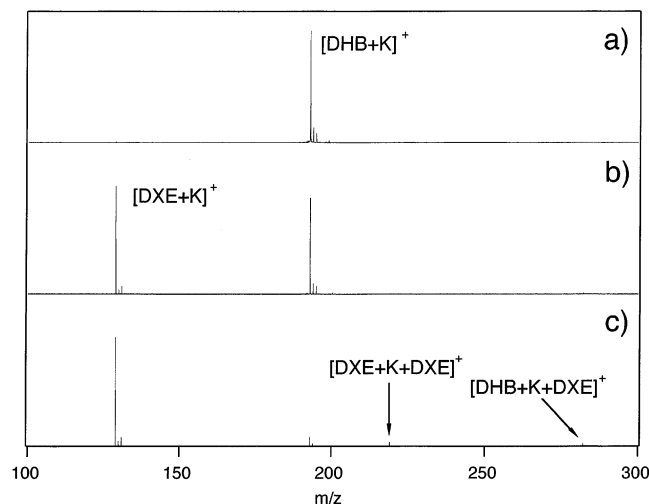


Figure 1. Positive ion mode FT ICR mass spectra of potassium cation transfer reactions between potassiated 2,5-dihydroxybenzoic acid and 1,2-dimethoxyethane after (a) 2 μ s, (b) 5 s, and (c) 35 s reaction time.

between potassiated DHB and 1,2-dimethoxyethane (DXE); at the beginning of the reaction (a), with 6 s reaction time (b), and at the reaction equilibrium (c). In contrast to the sodium transfer reactions studied in a previous work,⁴² the metal ion bound hetero- and homodimers were barely observed in these potassium transfer reactions. Generally, only very minor amounts of homodimer [DXE + K + DXE]⁺ and heterodimer [M + K + DXE]⁺ (M is matrix molecule) were observed, as shown in Figure 1. This small amount of dimer does not affect the reaction equilibrium significantly, and was therefore ignored in this work.

In Figure 2a, the kinetics of the potassium transfer reaction is shown. For determining the gas-phase potassium basicity of DHB, the ion ratio at equilibrium was obtained as the average value of five measurements, [DHB + K]⁺/[DXE + K]⁺ = 5 ± 2 (Figure 2b). The ratio of neutrals [DHB]/[DXE] determined by EI was 0.06 ± 0.05. The free energy for the potassium transfer reaction from potassiated DHB to DXE is $\Delta G = 3 \pm 2$ kJ mol⁻¹. The reference value for eq 2 is taken from Sunner et al.,²² GKB(DXE) = 96 kJ mol⁻¹. The gas-phase potassium basicity of DHB is thus 99 ± 2 kJ mol⁻¹. The error may be larger (up to ±4 kJ mol⁻¹) than that given here, since no error for the reference value was given by Sunner et al.,²² and was therefore not included. Furthermore, the gas-phase potassium basicities of the other three matrices are 104 ± 3 kJ mol⁻¹ for sinapinic acid, 97 ± 4 kJ mol⁻¹ for 2,4,6-trihydroxyacetophenone, and 94 ± 3 kJ mol⁻¹ for dithranol.

Comparing the gas-phase sodium basicities (Table 1), a linear correlation is obtained. For both Na⁺ and K⁺ binding to the matrices, the order is SA > DHB > THAP > dithranol. Ryzhov et al. have also found that there is a linear correlation between Na⁺ and K⁺ binding to the aromatic amino acids.²⁷ This correlation may be because of the structure of the matrix

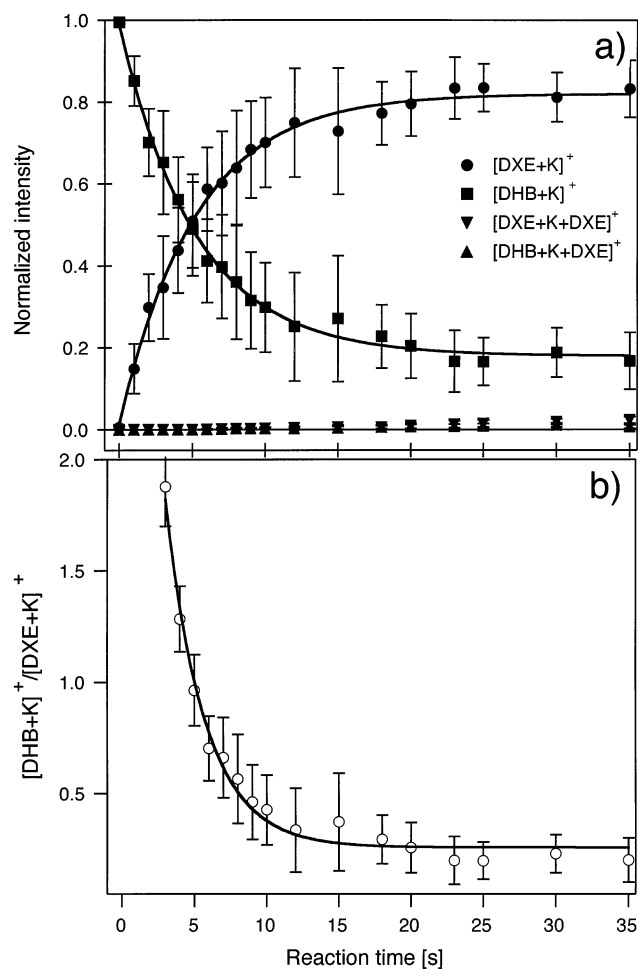


Figure 2. Kinetic plot of gas-phase potassium cation transfer reaction between potassiated 2,5-dihydroxybenzoic acid and 1,2-dimethoxyethane. (a) Plot of normalized intensities of observed ion species vs reaction time. The solid lines are exponential fit functions; (b) plot of the intensities ratio [DHB + K]⁺/[DXE + K]⁺ vs reaction time.

molecules. Both SA and DHB molecules contain carboxylic oxygens that are obviously better electron donors for the binding of Na⁺ and K⁺ than aromatic hydroxyl oxygens. Dithranol has only hydroxyl functional groups on the π -system, and it has the lowest gas-phase potassium and sodium cation binding energies among the four matrices. This leads to an electrostatic mode of Na⁺ and K⁺ binding. The relative order of the gas-phase sodium basicities of 11 matrices given in a previous publication⁴² can be thus expected to be the same for potassium.

Na⁺ binds more strongly to matrix than K⁺, which is typical for electrostatic interactions: smaller ions bind more strongly. This sequence is also reflected in the MALDI mass spectra, where the signals of sodiated quasi-molecular ions are in general more intense than the potassiated ones, unless the molecules analyzed have a particularly high affinity to potassium cations. A good example of using this principle for solving a typical MALDI problem is given by North et al.¹⁶ The authors have added lithium salts into their MALDI sample to minimize the interfering signals caused by Na⁺ and K⁺ in the analysis of complex mixtures of oligosaccharides. By adding lithium salt, signals of sodiated and potassiated molecules are suppressed. This is because the Li⁺ binding energies are in general higher than those of Na⁺ and K⁺, and the gas-phase cationization process is thermodynamically controlled.¹⁵

4.2. Computational Results. To have a comparison of the different computational methods, we first calculated the gas-

TABLE 2: Binding Energies of [DXE + K]⁺ Obtained Theoretically and Experimentally

methods	$-\Delta H^{298}$ (kJ mol ⁻¹)	$-\Delta G^{298}$ (kJ mol ⁻¹)
RHF/6-31+G* ^a	119.6	
RHF/6-31+G*//MP2/6-31+G* ^a	131.7	
MP2/6-31+G* ^a	130.8	
MP2/aug-cc-pVDZ ^a	125.4	
MP2/VTZ//MP2/est CBS ^a	133.8	
B3LYP/6-31+G* ^a	122.4	88.8
CID experiment ^b	120.4	
equilibrium experiment ^c	129.6	96.1

^a Ab initio results are taken from Hill et al.³⁷ ^{b,c} Experimental values obtained by the threshold collision induced dissociation method and equilibrium method are taken from More et al.²⁹ and Sunner et al.²² Values obtained by DFT method are from this work.

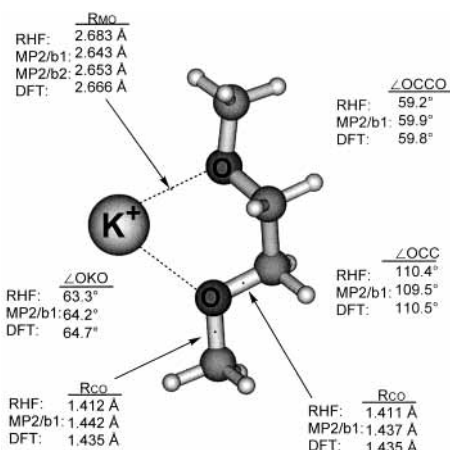


Figure 3. Optimized geometry of the [DXE + K]⁺ complex at the B3LYP/6-31+G* level (DFT). The geometry parameters obtained at the RHF/6-31+G*, MP2/6-31+G* (MP2/b1), and MP2/aug-cc-pVDZ (MP2/b2) are taken from Hill et al.³⁷

phase potassium binding energy of 1,2-dimethoxyethane using the DFT method at the B3LYP/6-31+G* level. This was done because the [DXE + K]⁺ complex has been well investigated experimentally and theoretically by ab initio methods at different levels, and also because 1,2-dimethoxyethane is the reference base employed in this work. The [DXE + K]⁺ complex has previously been studied by the equilibrium method,²² CID experiments,²⁹ and theoretical calculations.³⁷ The potassium binding energies of 1,2-dimethoxyethane obtained by different methods are given in Table 2. Among these, the only value of potassium binding free energy was determined experimentally by the equilibrium method ($\Delta G_{300} = 96.1$ kJ mol⁻¹).²²

Figure 3 shows the optimized geometry of the [DXE + K]⁺ complex and the structural parameters. The metal–oxygen distances (R_{MO}) are the most crucial parameters. Different computational methods and basis sets give the largest differences for this parameter. The potassium–oxygen distance obtained by DFT is 0.023 Å larger than that found by MP2/6-31+G*, and 0.013 Å larger than that obtained by MP2/aug-cc-pVDZ. The RHF gives the largest value among all the methods. In Table 2, all the calculated binding energies are fairly comparable with the experimental values. A better agreement is obtained by both RHF and DFT using the standard basis sets (6-31+G*) in comparison with the CID experiment results. For the MP2 theory, different basis sets give minor variations. The equilibrium method gives a higher binding energy than the CID experiment. They differ by 9.2 kJ mol⁻¹. If the average of the two experimental values is taken (125 kJ mol⁻¹), and compared

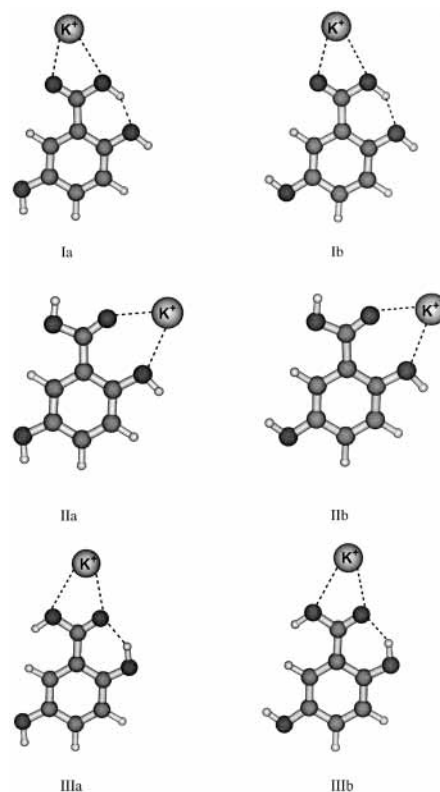


Figure 4. Optimized structures of the [DHB + K]⁺ complex at the B3LYP/6-31+G* level

with the theoretical values, the DFT method gives a good agreement, with only 2% deviation.

The MALDI matrices studied in this work have aromatic rings and carboxyl and hydroxyl functional groups. The competition between the π -system and those functional groups can result in number of binding conformations of the potassium cation. Two types of interactions in the K⁺–matrix complex may exist, namely, a charge–dipole interaction between K⁺ and the oxygens on functional groups, and the cation– π interaction between K⁺ and benzene ring. These interactions are largely electrostatic³⁴ in accord with conclusion of the experimental studies. Sodium cation binding to DHB and THAP has been studied previously,²⁰ which can provide some guidelines in terms of searching for the most stable conformations. The geometrical information of the most stable neutrals and the sodium complex in the case of DHB and THAP are taken from our previous work.²⁰ For SA and dithranol, the sodium complexation was also studied. The vibrational frequency calculations were carried out for all optimized geometries, to ensure that the optimized geometry of the potassium complexes give the true minima on the energy surface. The calculated vibrational frequencies with their IR intensities of the matrix molecules as well as their metal ion complexes in the most stable structure are summarized in tables submitted as Supporting Information.

DHB. There are many possibilities for potassium cation binding to DHB. By analogy to Na⁺,²⁰ the interaction between K⁺ and a single hydroxyl oxygen will certainly result in lower binding energy than if the potassium cation is bound to the carboxylic oxygens or to both a carboxylic oxygen and a hydroxyl oxygen. Figure 4 shows the different conformations of [DHB + K]⁺ considered in this work. In all structures, the potassium sits in the molecular plane of DHB. The structures in Figure 4 represent basically three types (I, II, III) of K⁺ binding to DHB. For each of these types, two different conformations result from the rotation of the 5-hydroxyl group

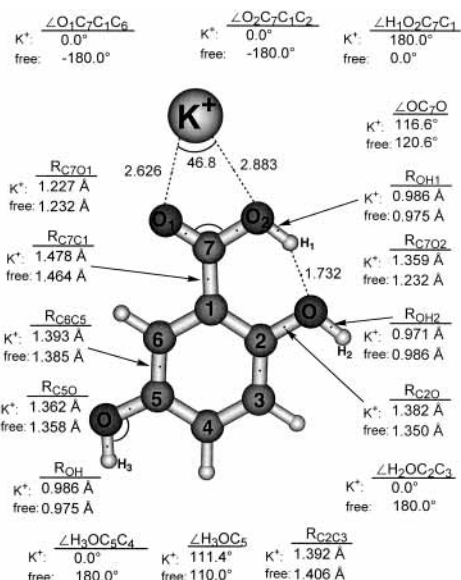


Figure 5. Detailed geometrical information of the [DHB+K]⁺ complex and the most stable neutral obtained at the B3LYP/6-31+G* level.

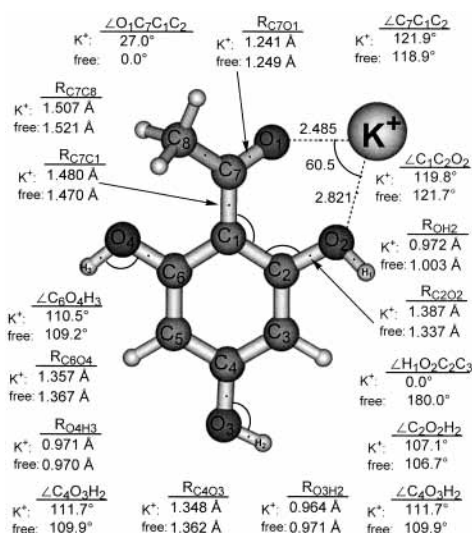


Figure 6. Detailed geometrical information of the [THAP+K]⁺ complex and the most stable neutral at the B3LYP/6-31+G* level.

(refer to Figure 5). “a” denotes structures with a dihedral angle $\angle H_3O_3C_5C_4 = 0^\circ$, whereas “b” stands for $\angle H_3O_3C_5C_4 = 180^\circ$. The most stable conformation of [DHB + K]⁺ is for K⁺ binding to the carboxyl group (structures **Ia** and **Ib**). **Ia** is slightly more stable than **Ib**, by 0.3 kJ mol⁻¹. If the structure **IIa** is compared to **IIb**, and **IIIa** to **IIIb**, respectively, the rotation of the 5-hydroxyl group costs 0.8 and 6.5 kJ mol⁻¹ energy. The calculated energies of the [DHB + K]⁺ complex and the relative energies with respect to the most stable one are given in Table 3. No local minimum was found for a cation- π interaction. The conformations of type **I** are more stable than type **II** and **III**, by about 7 and 18 kJ mol⁻¹. Detailed geometric information of the most stable [DHB + K]⁺ conformation (structure **Ia**) and the most stable structure of the neutral DHB are given in Figure 5. Potassium cation bound to the carboxylic oxygen gives the most stable structure of the complex, while sodium cation prefers to bind with both the carbonyl and the 2-hydroxyl oxygens.²⁰

THAP. The optimized geometry of the [THAP + K]⁺ complex and the detailed geometrical information are shown in Figure 6. Due to the symmetric environment of the acetyl

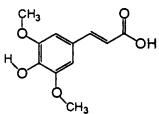
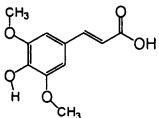
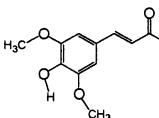
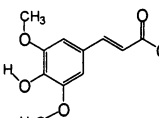
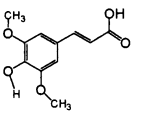
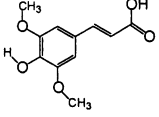
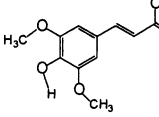
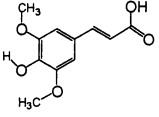
TABLE 3: Calculated Relative Energies with Respect to the Most Stable Structures for DHB, THAP, SA, and Dithranol, as Well as the Their Metal Cation Complexes in Different Conformers Obtained from Geometry Optimization at the B3LYP/6-31+G* Level

		<i>E</i> (a.u.)	ΔE (kJ mol ⁻¹)	
DHBK ⁺	Ia	-1171.0549926	0	
	Ib	-1171.0548852	0.3	
	IIb	-1171.0521968	7.3	
	IIa	-1171.0518788	8.2	
	IIIa	-1171.0481042	18.1	
	IIIb	-1171.0456121	24.6	
SA	IaN	-802.5103653	27.0	
	IIIaN	-802.5188218	4.8	
	IVaN	-802.5206364	0	
	Ia	-1402.2910201	0	
SAK ⁺	Ia	-1402.2907444	0.7	
	IIa	-1402.2897165	3.4	
	IVa	-1402.28925205	4.6	
	Ib	-1402.2872261	10.0	
	IIb	-1402.2873438	9.7	
	IIIb	-1402.2882259	7.3	
	IVb	-1402.2881723	7.5	
	SANA ⁺	Ia	-964.6672922	0.7
		IIa	-964.6669384	1.7
		IIIa	-964.6675707	0.0
		IVa	-964.667168	1.1
		Ib	-964.663322	11.4
IIb		-964.6632649	11.3	
dithranol	IIIb	-964.660652	18.2	
	IVb	-964.6661233	3.8	
	IaN	-765.2071263	33.7	
	IbN	-765.2199493	0.0	
dithranolK ⁺	IIaN	-765.2485562	54.6	
	IIbN	-765.2277653	0.0	
	Ia	-1364.9801984	0.0	
dithranolNa ⁺	Ib	-1365.0054296	0.0	
	IIb	-1364.9916338	36.2	
	Ia	-927.3601913	0.0	
	Ib	-927.3530827	18.7	
	IIa	-927.3858287	0.0	
	IIIb	-927.3597665	68.4	

group, only few possibilities exist for potassium cation binding to THAP. Apart from the binding to the single hydroxyl oxygen, the only likely potassium cation complexation of THAP that gives a considerable binding strength is given by binding to both the carbonyl and the 2-hydroxyl oxygens. No local minimum was found for the cation- π interaction. Attempted geometry optimization of a cation- π conformation formed no local minimum. The acetyl group rotates out of the molecular plane about the C₁-C₇ bond when binding to the potassium cation is established. This gives a torsion angle $\angle O_1C_7C_1C_2 = 27.0^\circ$.

SA. A more complex molecule such as sinapinic acid gives many more possibilities for binding to a cation. The neutral molecule also has many different stable conformations. Table 4 shows the calculated energies of the conformers of neutral sinapinic acid and the relative energies relative to the most stable conformer. In general, the cis-conformers are more stable than the trans-conformers. The energy for the conversion of cis and trans is 2 ~ 7 kJ mol⁻¹ depending on the conformation of other functional groups. The most stable conformation of the neutral sinapinic acid was found among the cis-conformers. The geometry optimization shows the same trends for the potassium and sodium cation complexes. The absolute and relative energies of the optimized potassium and sodium cation complexes are given in Table 3. The optimized structures of the metal cation (K⁺ and Na⁺) complexes, as well as the most stable neutral are shown in Figure 7. The labeling is based on the grouping of

TABLE 4: The Calculated Energies of the Optimized Structures of 3,5-Dimethoxy-4-hydroxycinnamic Acid and the Relative Energies with Respect to the Most Stable Structure at the B3LYP/6-31+G* Level

			SCF (a.u.)	Relative energy (kJ mol ⁻¹)
cis	1		-802.5206364	0
	2		-802.5205764	0.16
	3		-802.5188218	4.76
	4		-802.5186796	5.14
trans	5		-802.5196891	2.49
	6		-802.5195785	2.78
	7		-802.5165167	10.82
	8		-802.5157519	12.82

the cis- and trans-conformations (“a” denotes cis, whereas “b” denotes trans; refer to Table 3). In Figure 7, only the cis-conformers are shown. The corresponding neutrals of the complexes are labeled in analogy to the complexes and with an “N”. For example, the corresponding neutral of the structure **IVa** is **IVaN** (refer to Table 3). Although in most cases the corresponding neutrals possess higher energies than the most stable one, true local minima were found. This was proved by the vibrational frequency calculations. The importance of these corresponding neutrals will be discussed later in the section of comparison between experimental and theoretical results.

Due to lower stability of the trans-conformers, the cis-conformers were retained for further study. When the cation is bound to the carboxylic oxygens, structure **Ia** or **IIa** is formed. The 180° rotation of the 4-hydroxyl group distinguishes between structures **Ia** and **IIa**: **Ia** possesses a dihedral angle $\angle C_5C_4OH = 180.0^\circ$ and **IIa** possesses a dihedral angle $\angle C_5C_4OH = 0.0^\circ$, respectively (refer to Figure 8). The structures **III** and **IV** are obtained by the complexation of the cation with both methoxyl

and hydroxyl oxygens. The detailed geometrical information of the cation complexes and the most stable neutral is shown in Figure 8. The lengths of C–C bonds on the ring do not change significantly when complexes are formed, and therefore are not given. The cations remain in the SA molecular plane.

For K^+ , the most stable structure is **Ia**, whereas for Na^+ it is **IIIa**. In structure **Ia**, although the metal cation is bound at the end of the long chain, a change of bond length can be found also at the other end of the molecule, for instance, the length of O–C₄ bond. For the complexation of K^+ , the O–C₄ bond is shorter than that in the neutral SA. This is because the 4-hydroxyl group is involved in the complexation of K^+ by means of the conjugation. The arrows in Figure 8 show the migration path of the electron density via the conjugated system. The contribution of the 4-hydroxyl group in the complexation of K^+ (structure **Ia**) gives additional stability. In contrast to $[SA + K]^+$, the O–C₄ bond in $[SA + Na]^+$ is longer than that in the neutral SA. This indicates a charge-induced donation of the

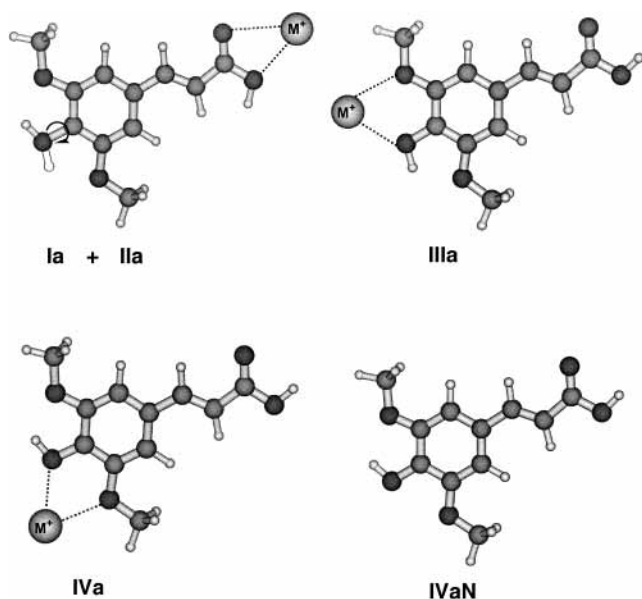


Figure 7. Optimized structures of $[SA + M]^+$ complexes ($M^+ = K^+$ and Na^+) and the most stable neutral of sinapinic acid obtained at the B3LYP/6-31+G* level.

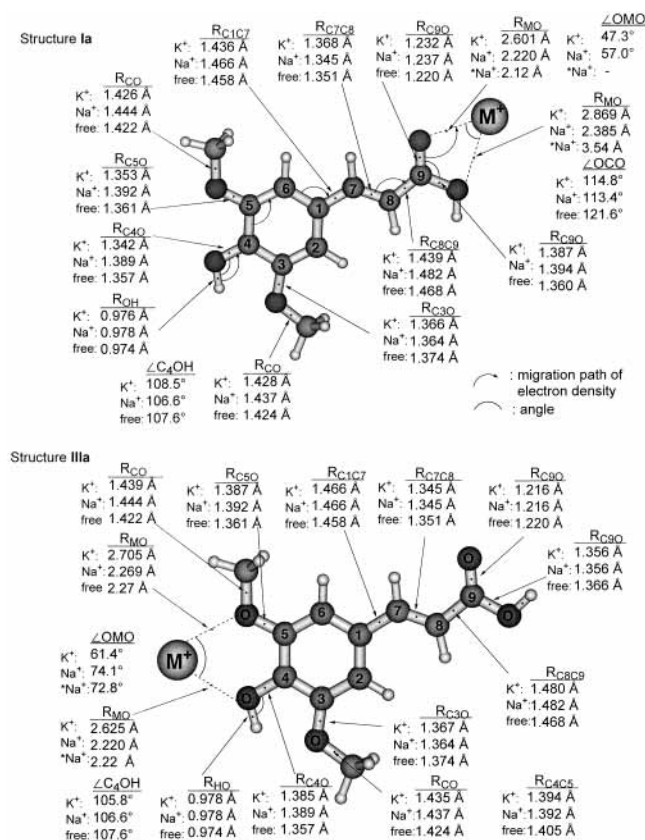


Figure 8. Detailed geometrical information of $[SA + M]^+$ complexes ($M^+ = K^+$ and Na^+) and the neutral sinapinic acid obtained at the B3LYP/6-31+G* level. The values with an asterisk are obtained at the HF/6-31G* level.¹⁹

electron density, which is weakened by increasing the bond distance, and is certainly less efficient than a conjugated system.

Ohanessian has studied the Na^+ complex of SA.¹⁹ The optimized geometries were obtained at the HF/6-31G* level. In this work, only the trans-configurations were considered. It was also found that the chelation of Na^+ by 4-hydroxyl and 3-methoxyl oxygens gives the most stable structure of the Na^+

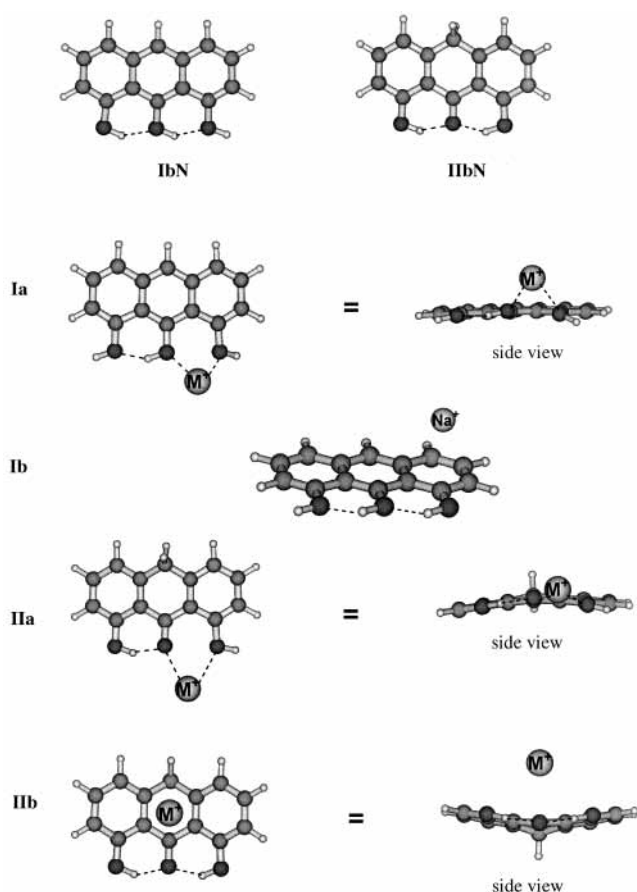
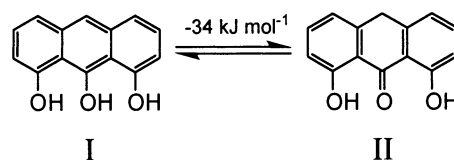


Figure 9. Optimized structures of $[dithranol + M]^+$ complexes ($M = K^+$ and Na^+) and the most stable neutral conformations for the two isomers obtained at the B3LYP/6-31+G* level.

complex. Among the trans-conformers, **IVb** is the most stable one (Table 3).

Dithranol. The dithranol used in the experiments is 1,8,9-trihydroxyanthracene. A stable tautomer of dithranol is 1,8-dihydroxy-9-anthrone.



It is interesting to compare the thermochemical properties of these two tautomers in the complexation of the sodium and potassium cations. We therefore included 1,8-dihydroxy-9-anthrone in the theoretical study. The optimized structures of the $[dithranol + M]^+$ complexes ($M^+ = K^+$ and Na^+), and the most stable neutral conformations are shown in Figure 9. "I" denotes the 1,8,9-trihydroxyanthracene, and "II" denotes the 1,8-dihydroxy-9-anthrone. Charge-dipole and cation- π interactions were considered. "a" stands for the chelation of the metal cations by oxygens, whereas "b" stands for the interaction between cations and the aromatic rings. The neutrals are again labeled after their corresponding complexes and marked with "N". For dithranol-I, no local minimum of the cation- π interaction was found for K^+ . In the case of Na^+ , a local minimum of the cation- π interaction was found with Na^+ over an end ring, where the electron density is obviously higher than the center. In contrast to dithranol-I, a local π -coordinated minimum was found for both K^+ and Na^+ in dithranol-II for

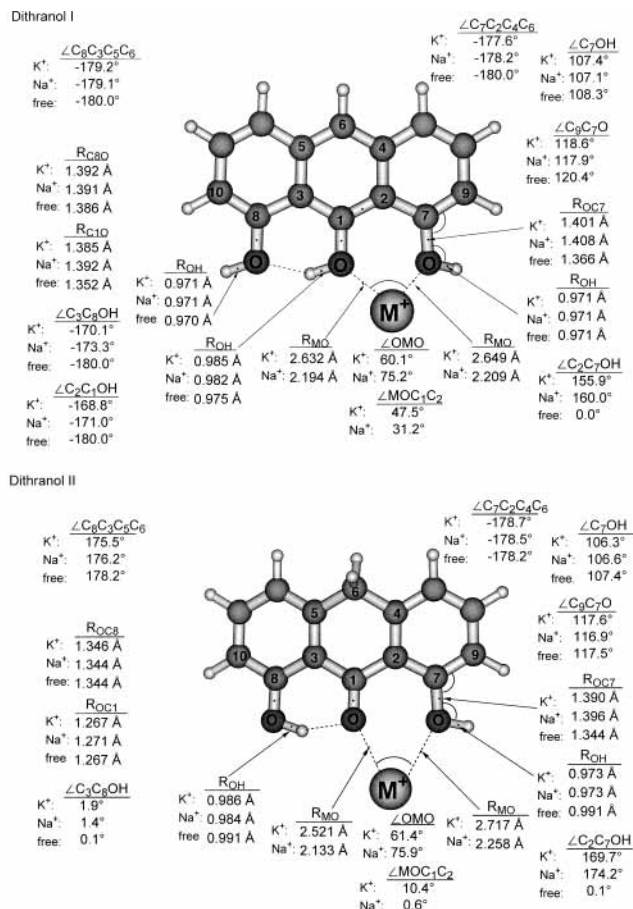


Figure 10. Detailed geometrical information of [dithranol + M]⁺ complexes (M = K⁺ and Na⁺) and the most stable neutral dithranol obtained at the B3LYP/6-31+G* level.

the metal cation over the middle ring. The most stable structure of the complex for both tautomers is, however, the binding of the metal cation by the chelation of two oxygens, as shown in Figure 9 (**Ia** for dithranol-I and **IIa** for dithranol-II). For the interaction of dithranol-I and K⁺, structure **Ia** is the only choice.

Detailed geometrical information on the most stable structure of the complexes and neutrals are given in Figure 10. The side view of structure **Ia** in Figure 9 shows that metal cations are too large to fit into the space between the two hydroxyl oxygens in the molecular plane. They are in fact over the molecular plane of dithranol with a dihedral angle $\angle\text{MOC}_1\text{C}_2 = 47.5^\circ$ for K⁺ and 31.2° for Na⁺. The 7- and 8-hydroxyl groups also rotate out of the molecular plane about the O–C₇ and O–C₈ bonds ($\angle\text{C}_2\text{C}_7\text{OH} = 155.9^\circ, 160.0^\circ$; and $\angle\text{C}_3\text{C}_8\text{OH} = -170.1^\circ, -173.3^\circ$ for K⁺ and Na⁺, respectively). The changes of the torsion angles for the left and right rings ($\angle\text{C}_7\text{C}_2\text{C}_4\text{C}_6$ and $\angle\text{H}_8\text{O}_3\text{C}_5\text{C}_6$) indicate a bending of the intact molecule slightly downward about the C₁–C₆ axis (from the side view).

The dithranol-II itself is somewhat arched and seems to be more flexible than dithranol-I. The bending of the molecule gives more space for the accommodation of the cations between two oxygens. The dihedral angles in this case are $\angle\text{MOC}_1\text{C}_2 = 10.4^\circ$ and for K⁺ and 0.6° Na⁺, much smaller than that in structure **Ia**. This can be clearly seen from the side view in Figure 9. For π -coordinated complexes (structure **Iib**), the intact dithranol molecule bends upward symmetrically. The R_{MC} is 3.633 and 3.374 Å for K⁺–C₆ and K⁺–C₁; 3.000 and 3.029 Å for Na⁺–C₆ and Na⁺–C₃, respectively.

Comparison with Experimental Results. The calculated metal cation binding energies of the matrices are given in Table 5.

TABLE 5: Gas-Phase M⁺ Binding Energies Obtained by the DFT Method at the 6-31+G* Level (298 K)^a

	A		B	
	$-\Delta G^{298}$	$-\Delta H^{298}$	$-\Delta G^{298}$	$-\Delta H^{298}$
[DHB+K] ⁺	69.4	96.4	107.5	138.5
[THAP+K] ⁺	58.9	85.8	116.1	158.9
[SA+K] ⁺ (Ia)	86.9	116.5	111.1	112.5
[SA+K] ⁺ (IIIa)	80.0	111.2	79.8	111.2
[SA+Na] ⁺ (IIIa)	132.5	165.8	132.3	165.8
[SA+Na] ⁺ (Ia)	135.6	168.1	159.9	194.0
[dithranol+K] ⁺ (Ia)	61.9	89.8	93.7	122.9
[dithranol+Na] ⁺ (Ia)	120.9	150.7	152.7	183.7
[dithranol+K] ⁺ (IIa)	51.4	79.7	101.6	131.9
[dithranol+Na] ⁺ (IIa)	113.7	142.6	163.8	195.9

^a The energies were obtained when the most stable complexes were compared with the most stable neutrals (column A), and when the most stable complexes were compared with their corresponding neutrals (column B). All the energies are in kJ mol⁻¹. Bold: the most stable conformation of the K⁺ (**Ia**) and Na⁺ complex (**IIIa**) of SA.

Column A contains the values obtained when the most stable structure of the complex is compared with the most stable structure of the neutral molecule, whereas the values in column B are obtained when the corresponding neutral of the complex is used for evaluating the binding energies. With the expression “corresponding neutral”, we mean that the neutral retains the same conformation as in the complex. All the energies are given in kJ mol⁻¹.

For DHB, $-\Delta H_A = 96.4$ kJ mol⁻¹, and $-\Delta G_A = 69.4$ kJ mol⁻¹, are obtained, if the most stable conformation of [DHB + K]⁺ is compared to the most stable conformation of the DHB neutral. The experimental K⁺ binding free energy of DHB is 99 ± 4 kJ mol⁻¹. The theoretical value is thus about 30 kJ mol⁻¹ lower than the experimental value (only the free energy values are compared). True energy minima were also found for the corresponding neutral DHB of the [DHB + K]⁺ complex. If the most stable conformation of [DHB + K]⁺ is compared to its corresponding neutral, the binding energies are $-\Delta H_B = 138.5$ kJ mol⁻¹ and $-\Delta G_B = 107.5$ kJ mol⁻¹. A much better agreement (9% deviation) is observed between the ΔG_B value and the experimental value. The corresponding neutral of the complex may not possess the most stable conformation, even though there is a local minimum on the potential surface. Obviously, there is an energy barrier for the conversion of the metastable conformation to the globally stable one.

In DHB and many other MALDI matrices, the functional groups are conjugated with the π -system of the benzene ring. This hinders the functional groups rotating out of the molecular plane. Single-point-energy calculations of the transition states (when the functional groups turn out of the molecular plane by about 90°) show that the rotation of the carboxyl group about C₁–C₇ bond costs 70 kJ mol⁻¹ energy. Also the rotation of the 2-hydroxyl functional group about the C₂–O bond takes 20 kJ mol⁻¹. These rotations are required for the relaxation of the metastable conformation to the most stable conformation. As discussed in our previous work,²⁰ the experiment was done with the ligand-exchange equilibrium method by observing the potassium cation transfer from the potassiated matrix molecule to the neutral reference base, as shown in reaction 3. After the potassium cation leaves the DHB, the neutral molecule may remain in the metastable conformation, since neither the thermal energy (at 298 K) nor the reaction energy (less than 10 kJ mol⁻¹) is sufficient to surmount these energy barriers. In this case, equilibrium may be established between the most stable complex and metastable neutrals. On the other hand, although there is a cooling process that ensures the reactants are at room temper-

ature, it might be possible to have a mixture of various conformations of the complex as reactant because of the small energy difference between some conformations of metal cation complex (e.g., the difference between **Ia** and **IIb** is only 7 kJ mol⁻¹).

A rotation of the 2-hydroxyl group is also required for conversion neutral THAP from the metastable conformation to the most stable conformation. A local minimum also exists for the corresponding neutral of the [THAP + K]⁺ complex. Values of $-\Delta G_A = 58.9$ kJ mol⁻¹, $-\Delta H_A = 85.8$ kJ mol⁻¹, and $-\Delta G_B = 116.1$ kJ mol⁻¹, $-\Delta H_B = 158.9$ kJ mol⁻¹ are obtained for THAP. The free energy value in column A is obviously too low in comparison with the experimental value of 97 ± 4 kJ mol⁻¹, whereas that in column B is a bit too high. Better agreement with less than 20% deviation is obtained between the experimental and the theoretical results when the corresponding neutral was used for evaluation of the theoretical binding energies.

A deviation of only 7% is obtained if the same comparison is made for the [SA + K]⁺ complex ($-\Delta G_{\text{exp}} = 104 \pm 4$ kJ mol⁻¹, $-\Delta G_B = 111.1$ kJ mol⁻¹). Structure **IIIa** gives a lower potassium binding free energy than structure **Ia** by at least 7 kJ mol⁻¹. This conformation (**IIIa**) is favored for sodium cation binding to sinapinic acid. Since the corresponding neutral conformation is very close to the most stable one (the energy difference between these two neutral conformations is only 0.2 kJ mol⁻¹), the final sodium binding energies are similar in columns A and B. This energy is 16% less than the experimental value ($-\Delta G_{\text{exp}} = 159 \pm 2$ kJ mol⁻¹). It is remarkable to see that the value obtained from conformer **Ia** in column B is $-\Delta G_B = 159.9$ kJ mol⁻¹. A deviation of only 1% is observed between theoretical and experimental values. The difference between these conformations in the [SA + Na]⁺ complex is only 0.7 kJ mol⁻¹. It is again very likely that a mixture of different conformations of both neutral and complex coexists and plays a role in the gas-phase cation transfer reaction. This assumption can be made for both potassium and sodium. The sodium binding energies of sinapinic acid obtained by the ab initio calculations at the MP2/6-311+G(2d,2p)//HF/6-31G* level¹⁹ are $-\Delta H^{298} = 163$ kJ mol⁻¹ and $-\Delta G^{298} = 128$ kJ mol⁻¹. These values are for the trans-conformer, which is less stable than the cis-conformer. They are about 3 kJ mol⁻¹ lower than our calculated values ($-\Delta H_B = 165.8$ kJ mol⁻¹, and $-\Delta G_B = 132.3$ kJ mol⁻¹).

The two tautomers of dithranol have differences of metal ion binding energies that are around 10 kJ mol⁻¹. We compared theoretical values of isomer **I** with our experimental values. As for the other matrices, a rotation of the 7-hydroxyl group about C₇-O bond is required for the relaxation of the corresponding neutral of the metal cation complex to the most stable neutral conformation. If the most stable complex (**Ia**) is compared with the corresponding neutrals for both K⁺ and Na⁺, metal ion binding free energies $-\Delta G_B = 93.7$ for K⁺ and 152.7 kJ mol⁻¹ for Na⁺ are obtained. Very good agreement is observed between the experiment ($-\Delta G_{\text{exp}} = 94 \pm 3$ for K⁺ and 150.5 ± 0.5 kJ mol⁻¹ for Na⁺) and theory with less than 1 and 2% deviation for K⁺ and Na⁺, respectively. The values in column A are again far too low in comparison with experimental results.

The different conformers of the [dithranol + K]⁺ and [dithranol + Na]⁺ complexes differ greatly in energy. For example, the conformer **IIa** (charge-dipole interaction, chelation) of the [dithranol + K]⁺ complex is 36 kJ mol⁻¹ (Table 3) more stable than the conformer **IIb** (cation- π interaction). In the case of [dithranol + Na]⁺, the difference between **IIa** and

IIb amounts to 68 kJ mol⁻¹. Unlike other matrices, the competition between different conformers of metal ion complex for dithranol is obvious, because there are different interactions involved. The structure of dithranol leads to the lowest gas-phase potassium and sodium basicities among all the MALDI matrices studied. The reason is that the interaction between the hydroxyl functional group and the sodium as well as potassium is much weaker than if the metal ion bound to the carboxylic functional group or to both carboxylic and hydroxyl functional groups as in the case of other matrices studied here.

Ohanessian has pointed out that attention must be paid to the comparison of the theoretical and experimental values obtained by the equilibrium method.¹⁹ The main argument is that the reference value used in the equilibrium method may influence the final results considerably. This is obviously unavoidable when employing this method in comparison, for example, with a CID experiment. However, the equilibrium method provides a rather good accuracy of relative values among all the different methods,⁶² in particular, in the investigation of the relative cation binding energies or proton affinities of a series of molecules, e.g., MALDI matrices, since systematic errors caused by all different kinds of factors including the reference value cancel out.

Consequences for MALDI Mass Spectra. The matrices studied in this work show different behaviors in binding of metal ions. This is mainly due to their structure and the functional groups they possess. In MALDI MS, dithranol is a well-known matrix used for polymer analysis, giving cationized analyte signals. In this work and two similar studies dealing with sodium ion binding energies of matrices,^{20,42} we found that dithranol has the lowest metal ion binding energy. For gas-phase cationization mechanism, no matter whether free cation attachment or cation transfer is predominant, matrix may compete with analyte for cations. The free energy of the cation transfer from matrix to analyte varies with different matrices. Among them, dithranol provides the highest exoergicity. This, according to the thermodynamic model, may explain why dithranol is the most suitable matrix when cationization is desired, as we have discussed in a previous report.⁴² Liao and Allison have reported that when SA is used as a matrix, no sodiated analyte signal can be detected.⁶³ Our results show that SA has the highest potassium binding free energy among the matrices studied. Its sodium binding free energy is also relatively high in comparison with the most other matrices. This may lead to a less intense sodiated analyte signal, although this hardly explains the complete absence of the sodiated analyte signal. The optimized geometry of [SA + M]⁺ (M = Na and K) in Figure 7 shows that metal ions can be bound to the hydroxyl and methoxyl oxygens besides the carboxylic oxygens. Both binding patterns give comparable sodium and potassium binding energies, resulting in the possibility for a multiply cationization of SA, i.e., [SA-H + 2M]⁺, which can sometimes also be observed in MALDI mass spectra. Other matrices such as DHB do not have this possibility. This may render SA even more competitive for cation binding in the MALDI plume.

5. Conclusions

(1) The gas-phase potassium binding free energies (potassium basicity GKB) of four MALDI matrices were measured by the ligand-exchange equilibrium method. The values of GKB were found to lie between 90 and 110 kJ mol⁻¹. The order of the GKBs for the matrices is SA > DHB > THAP > dithranol.

(2) The GKBs are less than GNABs by about 50 kJ mol⁻¹. A linear correlation between the GNAB and GKB was found, consistent with electrostatic considerations.

(3) The ligand-exchange equilibrium method gives reliable results for the relative values rather than the absolute values of binding energies.

(4) Theoretical studies of the structure and the binding energies of metal cation binding to MALDI matrices helps to better understand the experimental results. The metal ion complexes may have different conformations that coexist, because the energy differences between these conformers are low and activation energies for interconversion are high.

(5) Good agreements between the values obtained experimentally and theoretically were generally observed if the most stable conformation of the metal cation complex and its corresponding neutral were compared.

(6) The charge–dipole interactions between the functional groups on the benzene ring of MALDI matrices and the alkali metal ions play the main role in binding of metal ions. Matrices with carboxylic functional groups obviously have an advantage in the metal ion binding compared to matrices that only contain the hydroxyl functional groups, e.g., dithranol. Furthermore, the chelate coordination gives better binding of alkali metals.

Acknowledgment. This work has been funded by the Swiss Federal Institute of Technology. The generous allocation of computer time by the Informatikdienste der ETH Zürich (Stardust) and the Competence Center for Computational Chemistry (C4-cluster, ETH Zürich) is gratefully acknowledged.

Supporting Information Available: Tables showing the calculated vibrational frequencies with their IR intensities of the matrix molecules as well as their metal ion complexes in the most stable structure. This material is available free of charge via the Internet at <http://pubs.acs.org>.

References and Notes

- Belu, A. M.; DeSimone, J. M.; Linton, R. W.; Lange, G. W.; Friedman, R. M. *J. Am. Soc. Mass Spectrom.* **1996**, *7*, 11.
- Knochenmuss, R.; Lehmann, E.; Zenobi, R. *Eur. Mass Spectrom.* **1998**, *4*, 421.
- Cheng, H.; Clark, P. A. C.; Hanton, S. D.; Kung, P. *J. Phys. Chem. A* **2000**, *104*, 2647.
- Mowat, I. A.; Donovan, R. J.; Maier, R. R. *J. Rapid Commun. Mass Spectrom.* **1997**, *11*, 89.
- Rashidezadeh, H.; Hung, K.; Guo, B. *Eur. Mass Spectrom.* **1998**, *4*, 429.
- Nielen, M. W. F. *Mass Spectrom. Rev.* **1999**, *18*, 309.
- Rashidezadeh, H.; Guo, B. *J. Am. Soc. Mass Spectrom.* **1998**, *9*, 724.
- Rashidezadeh, H.; Wang, Y.; Guo, B. *Rapid Commun. Mass Spectrom.* **2000**, *14*, 439.
- Skelton, R.; Dubois, F.; Zenobi, R. *Anal. Chem.* **2000**, *72*, 1707.
- Wang, B. H.; Dreisewerd, K.; Bahr, U.; Karas, M.; Hillenkamp, F. *J. Am. Soc. Mass Spectrom.* **1993**, *4*, 393.
- Lehmann, E.; Knochenmuss, R.; Zenobi, R. *Rapid Commun. Mass Spectrom.* **1997**, *11*, 1483.
- Hoberg, A.-M.; Haddleton, D. M.; Derrick, P. J. *Eur. Mass Spectrom.* **1997**, *3*, 471.
- Belov, M. E.; Myatt, C. P.; Derrick, P. J. *Chem. Phys. Lett.* **1998**, *284*, 412.
- Zenobi, R.; Knochenmuss, R. *Mass Spectrom. Rev.* **1998**, *17*, 337.
- Knochenmuss, R.; Stortelder, A.; Breuker, K.; Zenobi, R. *J. Mass Spectrom.* **2000**, *35*, 1237.
- North, S.; Okafo, G.; Birrell, H.; Haskins, N.; Camilleri, P. *Rapid Commun. Mass Spectrom.* **1997**, *11*, 1635.
- Botek, E.; Debrun, J. L.; Hakim, B.; Morin-Allory. *Rapid Commun. Mass Spectrom.* **2001**, *15*, 273.
- Knochenmuss, R.; Zenobi, R. *Chem. Rev.* **2003**, *103*, 441.
- Ohanessian, G. *Int. J. Mass Spectrom.* **2002**, *219*, 577.
- Zhang, J.; Ha, T.-K.; Knochenmuss, R.; Zenobi, R. *J. Phys. Chem. A* **2002**, *106*, 6610.
- Sunner, J.; Nishizawa, K.; Kebarle, P. *J. Phys. Chem.* **1981**, *85*, 1814.
- Sunner, J.; Kebarle, P. *J. Am. Chem. Soc.* **1984**, *106*, 6135.
- Davidson, W. R.; Kebarle, P. *J. Am. Chem. Soc.* **1976**, *98*, 6133.
- Davidson, W. R.; Kebarle, P. *Can. J. Chem.* **1976**, *54*, 2594.
- Davidson, W. R.; Kebarle, P. *J. Am. Chem. Soc.* **1976**, *98*, 6125.
- Cerda, B. A.; Wesdemiotis, C. *J. Am. Chem. Soc.* **1996**, *118*, 11884.
- Ryzhov, V.; Dunbar, R. C.; Cerda, B. A.; Wesdemiotis, C. *J. Am. Chem. Soc.* **2000**, *11*, 1037.
- Klassen, J. S.; Anderson, S. G.; Blades, A. T.; Kebarle, P. *J. Phys. Chem.* **1996**, *100*, 14218.
- More, M. B.; Ray, D.; Armentrout, P. B. *J. Phys. Chem. A* **1997**, *101*, 4254.
- More, M. B.; Ray, D.; Armentrout, P. B. *J. Am. Chem. Soc.* **1999**, *121*, 417.
- Amunugama, R.; Rodgers, M. T. *Int. J. Mass Spectrom. Ion Proc.* **2000**, *195/196*, 439.
- Iceman, C.; Armentrout, P. B. *Int. J. Mass Spectrom.* **2003**, *222*, 329.
- Amunugama, R.; Rodgers, M. T. *Int. J. Mass Spectrom.* **2003**, *222*, 431.
- Ma, J. C.; Dougherty, D. A. *Chem. Rev.* **1997**, *97*, 1303.
- Hill, S. E.; Glendening, E. D.; Feller, D. *J. Phys. Chem. A* **1997**, *101*, 6125.
- Hoyau, S.; Ohanessian, G. *Chem. Eur. J.* **1998**, *4*, 1561.
- Hill, S. E.; Feller, D.; Glendening, E. D. *J. Phys. Chem. A* **1998**, *102*, 3813.
- Rodgers, M. T.; Armentrout, P. B. *Int. J. Mass Spectrom.* **1999**, *185–187*, 359.
- Dang, L. X. *J. Chem. Phys.* **2000**, *113*, 266.
- Hoyau, S.; Pélicier, J.-P.; Rogalewicz, F.; Hoppilliard, Y.; Ohanessian, G. *Eur. J. Mass Spectrom.* **2001**, *7*, 301.
- Rodgers, M. T.; Armentrout, P. B. *Mass Spectrom. Rev.* **2000**, *19*, 215.
- Zhang, J.; Knochenmuss, R.; Stevenson, E.; Zenobi, R. *Int. J. Mass Spectrom.* **2002**, *213*, 237.
- Curtiss, L. A.; Raghavachari, K.; Trucks, G. W.; Pople, J. A. *J. Chem. Phys.* **1991**, *94*, 7221.
- Bouchonnet, S.; Hoppilliard, Y. *Rapid Commun. Mass Spectrom.* **1993**, *7*, 470.
- Hill, S. E.; Feller, D. *Int. J. Mass Spectrom.* **2000**, *201*, 41.
- Hill, S. E.; Feller, D. *J. Phys. Chem. A* **2000**, *104*, 652.
- Hay, B. P.; Wadt, W. R. *J. Chem. Phys.* **1985**, *82*, 299.
- Rodgers, M. T.; Armentrout, P. B. *J. Am. Chem. Soc.* **2000**, *122*, 8548.
- Glendening, E. D.; Feller, D.; Thompson, M. A. *J. Am. Chem. Soc.* **1994**, *116*, 10657.
- Feller, D.; Glendening, E. D.; Woon, D. E.; Feyereisen, M. W. *J. Chem. Phys.* **1995**, *103*, 3526.
- Curtiss, L. A.; Redfern, P. C.; Raghavachari, K.; Pople, J. A. *J. Chem. Phys.* **1998**, *109*, 42.
- Feller, D.; Apra, E.; Nichols, J. A.; Bernholdt, D. E. *J. Chem. Phys.* **1996**, *105*, 1940.
- Dunbar, R. C. *J. Phys. Chem. A* **2002**, *106*, 7328.
- Bourcier, S.; Hoppilliard, Y. *Int. J. Mass Spectrom.* **2002**, *217*, 231.
- Bourcier, S.; Bouchonnet, S.; Hoppilliard, Y. *Int. J. Mass Spectrom.* **2001**, *210/211*, 59.
- Kinsel, G. R.; Knochenmuss, R.; Setz, P.; Land, C. M.; Goh, S.-K.; Archibong, E. F.; Hardesty, J. H.; Marynick, D. S. *J. Mass Spectrom.* **2002**, *37*, 1131.
- Becke, A. D. *J. Chem. Phys.* **1993**, *98*, 5648.
- Becke, A. D. *J. Chem. Phys.* **1993**, *98*, 1372.
- Lee, C.; Yang, W.; Parr, R. G. *Phys. Rev. B.* **1988**, *37*, 785.
- Boys, S. F.; Bernadi, F. *Mol. Phys.* **1993**, *19*, 553.
- Frisch, M. J.; Trucks, G. W.; Schlegel, H. B.; Scuseria, G. E.; Robb, M. A.; Cheeseman, J. R.; Zakrzewski, V. G.; Montgomery, J. A., Jr.; Stratmann, R. E.; Burant, J. C.; Dapprich, S.; Millam, J. M.; Daniels, A. D.; Kudin, K. N.; Strain, M. C.; Farkas, O.; Tomasi, J.; Barone, V.; Cossi, M.; Cammi, R.; Mennucci, B.; Pomelli, C.; Adamo, C.; Clifford, S.; Ochterski, J.; Petersson, G. A.; Ayala, P. Y.; Cui, Q.; Morokuma, K.; Malick, D. K.; Rabuck, A. D.; Raghavachari, K.; Foresman, J. B.; Cioslowski, J.; Ortiz, J. V.; Stefanov, B. B.; Liu, G.; Liashenko, A.; Piskorz, P.; Komaromi, I.; Gomperts, R.; Martin, R. L.; Fox, D. J.; Keith, T.; Al-Laham, M. A.; Peng, C. Y.; Nanayakkara, A.; Gonzalez, C.; Challacombe, M.; Gill, P. M. W.; Johnson, B. G.; Chen, W.; Wong, M. W.; Andres, J. L.; Head-Gordon, M.; Replogle, E. S.; Pople, J. A. Gaussian 98, revision A.9; Gaussian, Inc.: Pittsburgh, PA, 1998.
- Witt, M.; Grützmacher, H.-F. *Int. J. Mass Spectrom.* **1997**, *164*, 93.
- Liao, P.-C.; Allison, J. *J. Mass Spectrom.* **1995**, *30*, 408.